

Charge transport in superconductor/semiconductor/normal-conductor step junctions

S. G. Lachenmann, I. Friedrich, A. Förster, D. Uhlisch, and A. A. Golubov*

Institut für Schicht- und Ionentechnik, Forschungszentrum Jülich, D-52425 Jülich, Germany

(Received 14 February 1997; revised manuscript received 4 June 1997)

We present experimental data on the transport properties of a two-dimensional electron gas in contact with a superconducting and a normal conducting electrode. A short distance (≈ 500 nm) between the electrodes is realized by means of a step geometry. At voltages below the gap voltage of the superconductor, a decrease in resistivity of about 10% is observed. At low temperature and for voltages corresponding to a value smaller than the Thouless energy, an enhancement of the resistance is observed. The resistance at low energy coincides approximately with the resistance value above the gap voltage and depends sensitively on the bias current, temperature, and magnetic field. The experimental results are compared to theories of the reentrance effect. For small energies, good agreement is found. [S0163-1829(97)03245-1]

I. INTRODUCTION

Mesoscopic structures in which normal metal wires, semiconductors, or a two-dimensional electron gas (2DEG) are attached to superconductors have received much attention in the past few years (see, e.g., Ref. 1). In this article, experimental results on the transport properties of a 2DEG (in the dirty limit) are presented. On the one side, the 2DEG is brought in direct contact with a superconducting reservoir. On the other side, the 2DEG is connected to a normal conducting reservoir by means of a highly transparent contact. Such a junction is just a particular example of a nonequilibrium superconductor: First, superconducting correlation penetrates into the 2DEG and the Cooper pair amplitude is non-zero there. Second, an applied voltage results in a penetration of the electric field into the 2DEG and the quasiparticle distribution function is driven out of equilibrium.

Figure 1 shows a sketch of a superconductor (S)/normal-conductor (N) junction considered here. A 2DEG (or mesoscopic metal N') is connected by means of highly transparent boundaries to a S and a N electrode. A short distance between the S and N electrodes is necessary, since phase coherence of the charge carriers has to be maintained. In this article, a short distance L of approximately 500 nm between the electrodes is realized by a step geometry.

Normal-superconductor junctions have already been investigated theoretically in the 1970s by Artemenko, Volkov, and Zaitsev.² They predicted that at zero energy (temperature $T=0$ and bias voltage $V=0$) the total resistance of the S-N junction coincides exactly with a junction using two normal conducting electrodes (N-N junction). With increasing T , the resistance of the S-N junction is first decreasing, and then increasing again. For high T , it reaches its normal state value. This phenomenon is called the thermal proximity effect or reentrance effect.

A further understanding of this effect has been achieved very recently by several authors.³⁻⁵ The physics behind this reentrance effect involves nonequilibrium effects between quasiparticles injected by the N reservoir and electron pairs leaking from S. Volkov *et al.*³ propose that particle-hole symmetry breaking due to the use of a small but finite bias voltage provides a mechanism for the reentrance effect, even

at zero temperature. Nazarov and Stoof⁴ attribute the reentrance behavior of the resistivity to an energy dependence of the diffusivity in N' . In Ref. 5, it is proposed that the reentrance effect is due to a soft pseudogap in the density of states in the N' -metal. Despite the different models, all mentioned theories³⁻⁵ describe different aspects of the same phenomenon, whose existence arises from the phase-coherent nature of Andreev scattering. All these various approaches predict a decrease of the system's resistance of about 10% for voltages below the gap voltage Δ/e of the superconductor, where e is the elementary charge. If all energies involved are smaller than the Thouless energy $\varepsilon_g = \hbar D/L^2$, the resistance will increase again with decreasing energy (with decreasing T or V) (\hbar is Planck's constant divided by 2π , and the characteristic energy scale ε_g is inversely proportional to the time it takes for an electron to diffuse across the length L with diffusion coefficient D). At $T=0$ and $V=0$ the resistance coincides exactly with the resistance without the influence of the superconductor. All mentioned theories³⁻⁵ assume that charge transport in N' is in the diffusive limit, which implies that L needs to be much larger than the elastic mean free path l_{el} of the charge carriers. If the condition $L/l_{el} \gg 1$ is not fulfilled, the contact resistance R_c between S and N' must be taken into account. R_c is predicted to be voltage and magnetic field dependent.^{6,7}

To obtain an understanding of the physics behind the reentrance behavior of the system's resistance, we give a short

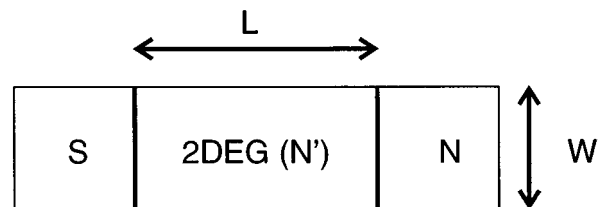


FIG. 1. Sketch of the junction considered here. A 2DEG (or mesoscopic normal metal N') is connected by means of highly transparent boundaries to a superconducting (S) and a normal conducting (N) electrode. The distance between the electrodes is L , and W is the width of the junction.

summary of the theory presented in Ref. 5. The proximity induced superconducting correlation between electrons in a diffusive normal metal N' survives up to a distance of order $\xi_N \propto \sqrt{D/T}$ (normal coherence length), where D is the diffusion coefficient in N' and T the temperature. When T is reduced, the proximity induced superconductivity expands in the normal metal N' , and the resistance of the system is decreased. At sufficiently low T , the length ξ_N becomes of the order of the size L of the normal layer N' . Now, the system's behavior becomes sensitive to the influence of the N electrode. If the boundary between the N electrode and the N' area is highly transparent, the reentrance effect appears. It can be shown,⁵ that the spatially averaged density of states in the N' area shows a soft pseudogap which is of the order of ε_g . This means that the density of states in N' at small energies $\varepsilon < \varepsilon_g$ is smaller than its normal state value (without the influence of S), but always remains nonzero. It increases with increasing ε and reaches its normal state value for $\varepsilon \geq \varepsilon_g$ (see Fig. 7 in Ref. 5). Therefore, with increasing ε ($\varepsilon < \varepsilon_g$), the system's resistance is decreasing. Since in the presence of proximity-induced superconductivity correlated and uncorrelated electrons contribute to the current, the system's resistance in the case of fully transparent interfaces is never larger than its normal state value (N-N junction). For $\varepsilon = 0$ ($T = 0$ and $V = 0$) it coincides exactly with its normal state value.

All calculations presented in Refs. 3–5 consider the “narrow” junction limit, where the width W of the normal conductor N' (see Fig. 1) is smaller than ξ_N . For the thin film geometry ($W \gg L$), which describes the system presented in this article more closely, no complete theory exists yet. However, if the current distribution in the junction is homogeneous, we expect no qualitative difference between two-dimensional and quasi-one-dimensional theory. The geometry of the junctions, which will be discussed here, is close to “overlap” geometry for Josephson tunnel junctions. For overlap junctions it is shown that the current is distributed almost uniformly (see, e.g., Ref. 8).

The low-temperature reentrant behavior of the resistance has been measured very recently by Charlat *et al.*^{9,10} and Petrashov *et al.*¹¹ They used disordered normal metal structures containing superconducting islands or boundaries. Charlat *et al.* demonstrated that a normal conducting Cu wire, which is connected to a superconducting and a normal conducting reservoir, shows a reentrance effect for energies smaller than ε_g . The authors have shown that this phenomenon can be observed in the differential resistance as a function of temperature and as a function of the bias current, respectively. The characteristic voltage V_g is related to ε_g by $V_g \approx \varepsilon_g/e$, and the characteristic temperature T_g by $T_g \approx \varepsilon_g/k_B$, where k_B is Boltzmann's constant. The experiments of Petrashov *et al.*¹¹ have shown that the amplitude of $h/2e$ oscillations in the magnetoresistance of a mesoscopic normal metal ring with two superconducting “mirrors” drastically differs in magnitude from that of the ring without superconductors. The oscillation amplitude is maximal at a temperature corresponding to the Thouless energy (ε_g/k_B). Closely related to the low-temperature reentrant behavior are recent results obtained by tunneling spectroscopy experiments with mesoscopic wires in contact with normal and superconducting electrodes by Guéron *et al.*¹²

In this article, a 2DEG is employed as the mesoscopic material N' between the S and N electrodes. Charge transport in the 2DEG is considered to be in the “clean limit,” if the elastic mean free path l_{el} is larger than ξ_N , whereas it is in the dirty limit for $l_{el} \ll \xi_N$. If l_{el} is larger than the sample length L , charge transport in the junction is ballistic, whereas it is diffusive for $l_{el} < L$. Here, charge transfer in the 2DEG is diffusive, as revealed from transport measurements discussed in Sec. II.

Experiments where a 2DEG is coupled to closely spaced S and N electrodes have been reported very recently by den Hartog *et al.*¹³ There, a reentrance behavior in the temperature dependence of magnetoresistance oscillations is observed. In contrast to this experiment, we have used a different sample configuration and a different material. Here, the reentrance behavior in a 2DEG is measured directly in the differential resistance as a function of temperature, bias current, and magnetic field.

II. SAMPLES

Hybrid junctions which combine superconductors and a 2DEG can be fabricated from Nb and InAs (see, e.g., Refs. 14–16). Pinning of the Fermi level inside the conduction band at the surface of InAs allows free transport of electrons across the S/2DEG interface, thus avoiding a Schottky barrier. The surface of p -type InAs is characterized by a high-mobility inversion layer, which represents a 2DEG (see, e.g., Ref. 17). The 2DEG channel has a depth of approximately 10 nm. Step junctions (with two Nb electrodes) using the surface inversion layer of p -InAs as a two-dimensional channel between the electrodes have been proposed by Kastalsky.¹⁸

For the step junctions discussed here, a 300-nm-thick low- p -doped (p^-) epitaxial layer (acceptor concentration $n_p \approx 5 \times 10^{16}/\text{cm}^3$) is grown on a highly- p -doped (p^+) substrate ($n_p \geq 10^{18}/\text{cm}^3$) using molecular beam epitaxy (MBE). At $T = 4.2$ K the hole density in the p^- layer is reduced due to freeze-out, so that the conductivity is entirely controlled by the surface 2DEG. The parameters of the 2DEG inversion layer have been investigated using a Corbino geometry,¹⁹ where ring-shaped Au electrodes on top of InAs are used to apply the current and to measure the voltage. The existence of the surface 2DEG has been confirmed by Shubnikov–de Haas measurements at $T = 1$ K, yielding an electron concentration in the 2DEG of $n \approx 10^{12}/\text{cm}^2$. By analyzing the dependence of the differential resistance dV/dI on an applied magnetic field B the mobility μ of the inversion electrons is estimated to be $\mu \approx 5000$ $\text{cm}^2/\text{V s}$. The sheet resistance R_{\square} at $T = 1.2$ K is $R_{\square} \approx 1.16$ $\text{k}\Omega$.²⁰ From these values, the elastic mean free path is estimated to be $l_{el} = v_F \tau \approx 78$ nm, with the Fermi velocity $v_F = \hbar k_F / m^* \approx 1.2 \times 10^6$ m/s and scattering time $\tau = m^* \mu / e \approx 65$ fs. [$k_F = \sqrt{2\pi n}$ is the Fermi wave vector. The effective mass in InAs m^* is assumed to be $m^* \approx 0.023 m_e$ (see, e.g., Ref. 17), where m_e is the free electron mass.] The diffusion constant is $D = (1/2)v_F l_{el} \approx 470$ cm^2/s . The superconducting correlation length in the 2DEG (“dirty limit”) is given by $\xi_N = \sqrt{(\hbar/2\pi k_B)(D/T)}$, yielding $\xi_N \approx 240$ nm at $T = 1$ K. According to literature (see, e.g., Ref. 21), the inelastic mean free path l_{in} in the surface inversion layer of

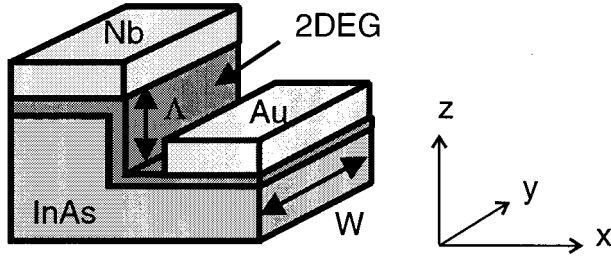


FIG. 2. Sketch of a Nb/Au step junction. The upper electrode is a Nb film, the lower electrode is a Au film. The dark area indicates the 2DEG at the surface of InAs. The step height is $\Lambda \approx 250$ nm, the width of the sample is $W = 100$ μm .

InAs is approximately 1 μm for $T \approx 2$ K.

In order to observe coherent charge transport through the 2DEG, the distance between the electrodes has to be smaller than the phase-breaking length l_ϕ . l_ϕ gives the length scale, on which electrons traveling along different paths can interfere. In our samples we estimate it to be $l_\phi \approx l_{\text{in}} (\approx 1$ $\mu\text{m})$.

Here, a small distance is realized by using a step geometry (see Fig. 2), which allows one to fabricate a short channel length L (smaller than 200 nm), even without the necessity of using electron beam lithography. Nb and Au are used as superconducting and normal reservoirs, respectively. The surface inversion layer of p -type InAs (2DEG) provides the coupling between the two reservoirs.

For the samples discussed here, the first Nb electrode is sputtered at a pressure of about 10^{-7} mbar. Prior to the deposition of the Nb film, the sample surface is cleaned by rf Ar-sputter cleaning (dc bias: 800 V, 10 s). After a lift-off process, the step in InAs (height Λ) is etched using the first (top) Nb electrode as an etch mask. A wet-chemical etch ($\text{H}_2\text{O}_2:\text{H}_3\text{PO}_4:\text{H}_2\text{O} = 1:1:38$) with an etching rate of about 100 nm/min was used. Finally, the second electrode (Au) is deposited by e -beam evaporation at a pressure of about 10^{-7} mbar using the first electrode as shadow mask. The thickness of the top Nb film is about 150 nm, and the thickness of the lower Au film is 60 nm. It is known^{22,23} that Ar bombardment can change the electronic properties of InAs. Millea *et al.*²² studied the effect of low-energy Ar bombardment on the surface conductivity of p -InAs. They showed that n as well as μ is increased after Ar cleaning. However, with the 2DEG of an InAs based quantum well structure,²³ μ is shown to decrease due to Ar cleaning. Thus, the electronic properties of the 2DEG underneath the top electrode are probably different from those measured on the untreated layer. Prior to deposition of the second electrode, no argon cleaning was used. Thus, the main part of the channel, namely, the 2DEG at the side of the step, is not influenced by Ar cleaning, since it is etched after deposition of the first Nb electrode.

Due to the fabrication process (underetching and shadow evaporation of the second electrode), the effective channel length L is larger than the etch depth Λ . With an etch depth $\Lambda \approx 250$ nm, the channel length between the normal and superconducting reservoirs is $L \approx 500$ nm, as estimated from scanning electron micrographs. For the following considerations, the parameters of the 2DEG (carrier density n and the

TABLE I. Parameters of samples Nos. 1–4. $W = 100$ μm and $L \approx 500$ nm. R_n is the normal resistance, R_{min} the minimal resistance, and V_{ZBM} the width of the zero-bias maximum in the differential resistance on the V axis, respectively. $(-, +)$ denotes the negative and positive voltage axes. $T = 800$ mK, and $B = 0$.

	No. 1	No. 2	No. 3	No. 4
R_n [Ω] $(-, +)$	1.14, 1.12	2.11, 2.07	1.2, 1.18	3.5, 3.48
R_n/R_{min} $(-, +)$	1.08, 1.05	1.06, 1.04	1.07, 1.05	1.06, 1.04
V_{ZBM} [μV]	≈ 200	≈ 200	≈ 220	≈ 210

mobility μ) determined from planar geometry are used. Weak Shubnikov–de Haas oscillations are detected in the magnetoresistance dV/dI of the Nb/Au step junctions as well. However, it is difficult to determine n and μ quantitatively from these measurements, since for the surface inversion layer of p -InAs only measurements in Corbino geometry yield reliable data. If we assume that the parameters of the 2DEG at the step do not deviate significantly from those measured in planar geometry, the channel length L is much larger than the elastic mean free path l_{el} ($L/l_{\text{el}} \approx 6$) but shorter than l_ϕ . Furthermore, L is larger than ξ_N for $T > 300$ mK, and the gap energy Δ of Nb ($\Delta \approx 1.45$ meV) exceeds the Thouless energy ε_g (≈ 130 μeV). This implies that the step junctions are in a mesoscopic regime.

III. RESULTS AND DISCUSSION

The experiments have been performed in He(3) and He(3)/He(4) dilution cryostats. A magnetic field can be applied either in x (perpendicular to the step) or in the z -direction (see Fig. 2). The differential resistance dV/dI has been measured by the lock-in technique; the sample was biased with an ac current $dI \approx 1$ μA with a frequency of 170 Hz in addition to the dc current I . The voltage signal dV was phase sensitively detected.

A. Zero-bias maximum in the differential resistance

We tested four similar samples with width $W = 100$ μm and $L \approx 500$ nm. The parameters of the samples (Nos. 1–4) are listed in Table I.

Figure 3 shows the voltage dependence of the differential resistance dV/dI of a Nb/Au step junction (sample No. 1) at $T = 300$ mK and $B = 0$. For voltages much larger than the superconducting gap of Nb, $|V| > \Delta/e \approx 1.45$ mV, the resistance has the value R_n^+ and R_n^- for the positive and negative voltage axes, respectively. The asymmetry $R_n^-/R_n^+ \approx 1.02$ may be caused by a small parallel contribution of conductivity through the bulk p -InAs.¹⁶ For voltages smaller than Δ/e the resistance drops to a value which is about 10% less than R_n . At low voltage $|V_{\text{ZBM}}| \approx 200$ μV , a sharp increase of the resistance is observed. The resistance at zero bias is indicated by R_0 . The vertical arrows in Fig. 3 indicate the energy gap voltage of Nb ($V_\Delta = \Delta/e \approx 1.45$ mV); the tilted arrows define the (half) width V_{ZBM} of the zero-bias-resistance maximum (ZBM).

At voltages well above Δ/e , the current varies linearly with voltage and extrapolates to a positive current value I_{exc} at $V = 0$. The occurrence of an excess current ($I_{\text{exc}} \approx 10$ μA)

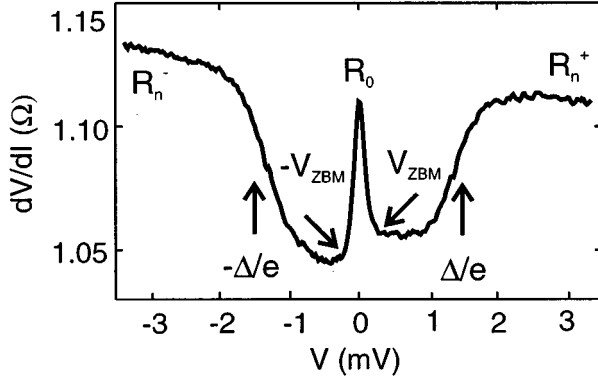


FIG. 3. Differential resistance dV/dI of a Nb/Au step junction as a function of the voltage V (Sample No. 1) at $T=300$ mK and $B=0$. The vertical arrows indicate the energy gap voltage of Nb ($V_\Delta = \Delta/e \approx 1.45$ mV), the tilted arrows define the (half) width V_{ZBM} ($\approx \pm 200$ μ V) of the zero-bias-resistance maximum.

indicates that the boundaries between the superconducting electrode and the 2DEG are highly transparent and that the boundary resistance is small.^{24,25}

For the step junctions with $L \approx 500$ nm and $D \approx 470$ cm²/s, $\varepsilon_g \approx 130$ μ eV is calculated. For all samples (Nos. 1–4, Table

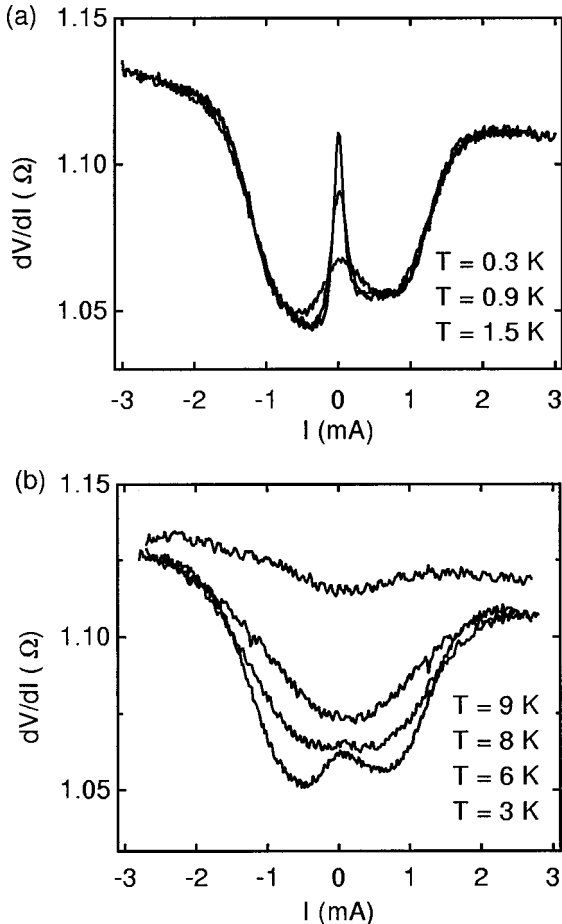


FIG. 4. (a), (b) Differential resistance dV/dI vs bias current I of sample No. 1 for different temperatures and $B=0$.

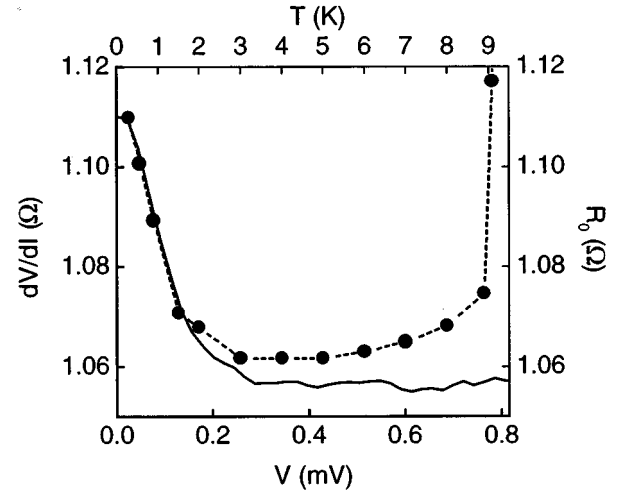


FIG. 5. Comparison of the temperature dependence of the zero-bias resistance R_0 with the voltage dependence of dV/dI at $T=300$ mK (sample No. 1). The solid circles indicate the measurement points of $R_0(T)$; the dashed line is only a guide for the eye (upper x axis, right y axis). The solid line is the measured $dV/dI(V)$ (lower x axis, left y axis). The x axes are related via $eV = k_B T$.

I), the width of the ZBM is $V_{ZBM} \approx 200$ μ V, which is approximately $1.6\varepsilon_g/e$. As will be shown in the next subsection, the temperature dependence of $R_0(T) = dV/dI(V=0, T)$ for small T is very close to the voltage dependence of the ZBM. Temperature and voltage can be related by $eV = k_B T$.

All four Nb/Au junctions on the same chip show qualitatively the same behavior (see Table I). With $W = 100$ μ m and $\Lambda \approx 250$ nm, the measured R_n is between 1 and 3.5 Ω .²⁶ The resistance decrease below the gap voltage is always about 10% of R_n . The resistance increases for voltages $|V| < |V_{ZBM}| \approx 200$ μ V. The dV/dI of all samples has an asymmetry of about 2%.

B. Temperature dependence of the zero-bias maximum

The height $R_0(T) = dV/dI(V=0, T)$ of the ZBM is decreasing with increasing temperature T . Figures 4(a) and 4(b) show the differential resistance of sample No. 1 for different T in dependence of the bias current I . For 300 mK $< T < 1.5$ K only the height $R_0(T)$ of the ZBM is decreasing, whereas no significant increase of the width of the ZBM (V_{ZBM}) can be detected. This is in accordance with the assumption, that the width of the ZBM is given by ε_g , which depends only weakly on T in this range. For $T > 3$ K the zero-bias resistance maximum is suppressed, and only a broad conductivity enhancement for $|V| < \Delta/e$ remains. For T larger than the critical temperature of Nb ($T_c \approx 9$ K), dV/dI is almost independent of V . The T dependence has to be compared with the situation under the influence of a magnetic field. A magnetic field yields a broadening of the ZBM, whereas the height R_0 is constant for small fields (see Sec. III D).

In Fig. 5, the experimentally observed temperature dependence of the zero-bias resistance R_0 is compared with the voltage dependence of dV/dI at $T=300$ mK. The upper x axis shows T ; the lower x axis shows V .

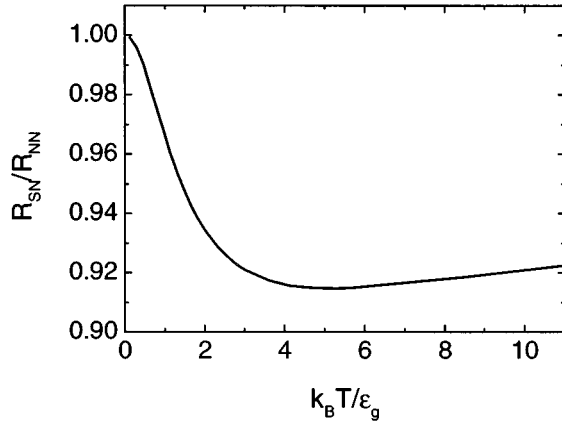


FIG. 6. Calculation of the resistance R_{SN} of a S-N'-N system as a function of T (after Ref. [5]) The resistance R_{SN} is normalized to its normal state value R_{NN} . T is normalized to ϵ_g/k_B .

The resistance enhancement is suppressed at a temperature of $2T_g \approx 2\epsilon_g/k_B \approx 3$ K. On the other hand, at low temperatures ($T < 3$ K), a voltage larger than approximately $1.6V_g \approx 1.6\epsilon_g/e \approx 200 \mu\text{V}$ suppresses the enhanced resistance. This comparison indicates again that ϵ_g is the relevant energy for the appearance of the zero-bias maximum. For small energies ($V < 300 \mu\text{V}$, $T < 3$ K), the T dependence of the ZBM corresponds very well to the V dependence of dV/dI . For $V > 300 \mu\text{V}$, the V dependence of dV/dI deviates from the T dependence of R_0 . This deviation will be discussed in the next section.

C. Temperature and voltage dependence of the zero-bias-resistance maximum: Comparison to theory

Figure 6 shows a calculation of the zero-bias resistance R_{SN} ($=R_0$) of a S-N'-N system (see Fig. 1) as a function of T . The calculation has been performed using the procedure described in Ref. 5. For this curve, it is assumed that no barrier between N (here Au) and N' (here 2DEG) exists. Furthermore, this calculation is based on the assumption that N' is in the diffusive limit ($L \gg l_{el}$) and that the superconducting energy gap is considerably larger than the Thouless energy ($\Delta \gg \epsilon_g$). As can be seen from Fig. 6, the resistance enhancement due to the reentrance effect appears approximately at $2\epsilon_g$. The experimental T dependence (Fig. 5) shows good qualitative agreement with the theory (Fig. 6) for $T < 6$ K. However, the predicted \sqrt{T} dependence of dV/dI for large T cannot be seen in our experiment. The reason for the discrepancy between experiment and theory for large T is that the theory assumes $\epsilon_g \ll \Delta$, whereas in our case $\epsilon_g \approx 1/7\Delta$.

The experimental voltage dependence of dV/dI (Fig. 5) shows good qualitative agreement with both the experimental and calculated T dependence of the zero-bias resistance (Fig. 5 and Fig. 6) for $V < 200 \mu\text{V}$. However, for $V > 300 \mu\text{V}$ the V -dependence deviates from both curves. This deviation can be explained in terms of the model of the reentrance effect given in Ref. 5. The expression for the current is given by Eq. (7) in Ref. 5:

$$I = \frac{1}{2R_n} \int_0^\infty d\epsilon \left[\tanh\left(\frac{\epsilon + eV}{2k_B T}\right) - \tanh\left(\frac{\epsilon - eV}{2k_B T}\right) \right] D(\epsilon). \quad (1)$$

Here $D(\epsilon)$ is the effective transparency of the system as introduced in Ref. 5, which in the absence of a barrier at the interface is determined by Eq. (17) of Ref. 5. The normalized conductance $\sigma(V, T) = (R_n dI/dV)$ in the two limiting cases of $T=0$ and $V=0$ is given by

$$\sigma(0, T) = \frac{1}{2k_B T} \int_0^\infty \frac{D(\epsilon)}{\cosh^2(\epsilon/2k_B T)} d\epsilon, \quad (2)$$

$$\sigma(V, 0) = D(eV).$$

An inspection of these expressions shows that due to the enhancement of the effective transparency of the system $D(\epsilon)$ at energies $\epsilon \sim \epsilon_g$ both quantities $\sigma(0, T)$ and $\sigma(V, 0)$ have maxima at $k_B T \sim \epsilon_g$ and $eV \sim \epsilon_g$ and show reentrant behavior, respectively. However, for comparable values $eV = k_B T$ the correction to the voltage-dependent conductivity is larger, i.e., $\delta\sigma(V, 0) > \delta\sigma(0, T)$.

This will be demonstrated now explicitly for the case $eV, k_B T \gg \epsilon_g$, when the high-energy asymptotics $D(\epsilon) = C\sqrt{\epsilon_g/\epsilon}$ gives the main contribution to $\delta\sigma$ (here C is the numerical constant calculated in Ref. 5). In this case, one immediately obtains $\delta\sigma(V, 0) = C\sqrt{\epsilon_g/eV}$, whereas $\delta\sigma(0, T) < C\sqrt{\epsilon_g/k_B T}$. Indeed, an upper estimate $\delta\sigma_{\max}(0, T) = C\sqrt{\epsilon_g/k_B T}$ follows assuming $\cosh^2(\epsilon/2k_B T) = 1$. Since at high energies ($\epsilon \gg k_B T$) the integral in Eq. (2) converges and $\cosh^2(\epsilon/2k_B T) > 1$, the above inequality follows in a straightforward way.

The physical reason for $\delta\sigma(V, 0) > \delta\sigma(0, T)$ is that in the calculation of $\delta\sigma(0, T)$ the whole Fermi distribution is taken into account and therefore the high-energy contribution to $D(\epsilon)$ is underestimated, whereas only electrons with $\epsilon = eV$ contribute to $\delta\sigma(V, 0)$.

This behavior is observed in the experiment. As can be seen from Fig. 5, $dV/dI(V)$ is smaller than $R_0(T)$ for $V > 200 \mu\text{V}$ and $T > 2$ K, respectively.

Another effect which might be superimposed to the reentrance effect is the voltage dependence of the contact resistance of the S-N' interface. According to Refs. 6 and 7, this effect plays a role if the condition $L/l_{el} \gg 1$ is not fulfilled (here $L/l_{el} \approx 6$). It is predicted,^{6,7} that application of either a voltage ($V \gg \epsilon_g/e$) or a magnetic field [$B \gg h/(eLW)$] reduces the contact resistance R_c in the NS junction by a factor of 2. However, R_c is not predicted to show any reentrance behavior. The voltage dependence of R_c would lead to a reduction of R_n , thus making the ratio $R_0/R_n > 1$ (see Fig. 29 in Ref. 7). Due to the asymmetry of the experimental curves, the effect of the voltage-dependent contact resistance cannot be observed clearly in our experiment.

D. Influence of a magnetic field

An applied magnetic field B (in the x direction) increases the width V_{ZBM} (or I_{ZBM}) of the reentrance peak. A small current range of dV/dI of sample No. 2 for different values of B is shown in Fig. 7(a). For $|B| < 2$ mT, no change of the width I_{ZBM} of the ZBM is detected. If B is increased above $|B| \approx 2$ mT, the width of the ZBM is increasing. Since the

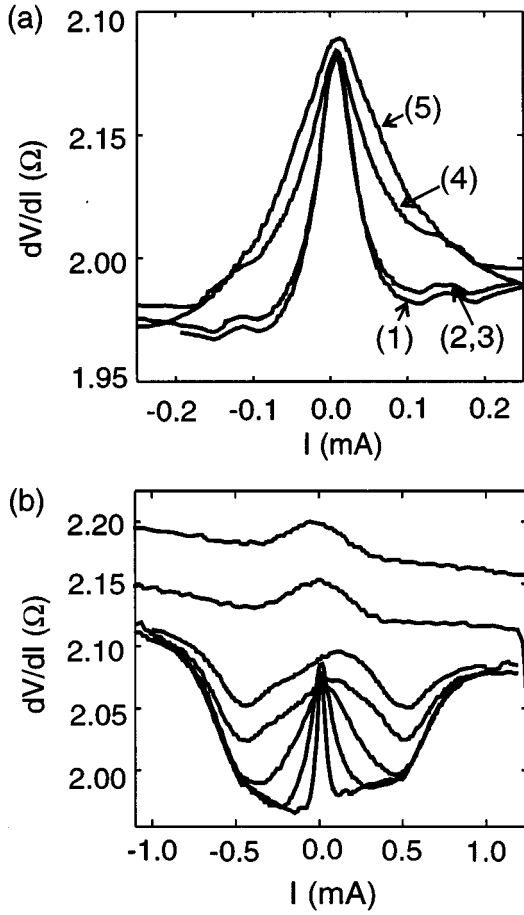


FIG. 7. (a) Differential resistance dV/dI of a Nb/Au step junction (sample No. 2) at different magnetic fields B . B is oriented perpendicular to the step (x direction). (1) 0 mT, (2,3) ∓ 2 mT, (4,5) ∓ 5 mT. (b) dV/dI of the same sample for a higher current and magnetic field range. From top to bottom: 1 T, 500 mT, 80 mT, 40 mT, 10 mT, 5 mT, and 0 mT.

step width in the setup to control the magnet used here is limited to 1 mT, we did not investigate the field dependence for $|B| < 1$ mT.

The differential resistance dV/dI of the same sample (No. 2) for a larger current range and for higher magnetic fields is shown in Fig. 7(b). The sharp ZBM broadens with B , and a gradual transition to a dV/dI curve with a broad, flat maximum around zero bias (resistance enhancement $\approx 1\%$) is observed. The shape of dV/dI for fields above $B = 500$ mT is very close to the dV/dI characteristics measured between electrodes on InAs, which have such a large distance ($> 10 \mu\text{m}$) that effects of phase coherence do not play a role anymore. The interplay between the inversion layer conductivity and the conductivity through the bulk p -InAs leads to a nonlinear current-voltage characteristics. A discussion of this nonlinear behavior of “macroscopic” InAs layers can be found, for example, in Refs. 20 and 30. This nonlinear shape of dV/dI remains up to about $T = 70$ K, and is only weakly field dependent. The increase of R_n in a magnetic field $B > 100$ mT is due to the increase of the resistance of InAs in a magnetic field.

An applied magnetic field suppresses the superconductivity in both S and the 2DEG. As shown in Figs. 7(a) and 7(b),

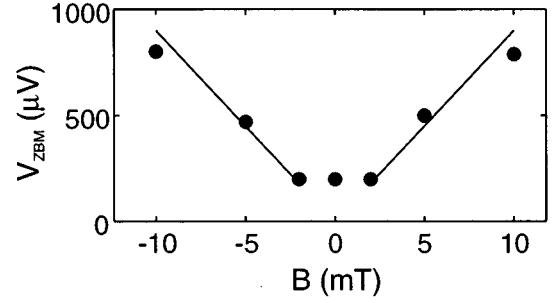


FIG. 8. Width V_{ZBM} of the zero-bias maximum (sample No. 2) as a function of the magnetic field B . The field is oriented in the x direction. $T = 1.2$ K. The circles indicate the measurement points; the solid lines are linear approximation curves (aB , with $a \approx \pm 90 \mu\text{eV/mT}$).

even for small fields, low enough to avoid any disturbance of the order parameter in S, the conductance of the S-2DEG-N structure is changed, especially at low voltages. To explain the broadening of the ZBM, we follow the arguments of Charlat *et al.*⁹ As an effect of the magnetic field B , the phase-memory length l_ϕ is decreasing. When l_ϕ becomes smaller than the sample length L , l_ϕ plays the role of an effective length L_{eff} for the sample. Since ε_g is proportional to $1/L_{\text{eff}}^2$, it is increased in a sufficiently high magnetic field. As a result, the resistance minimum is shifted to a higher voltage or, equivalently, the width of the ZBM is increased. This approach is supported by the observation that the width of the ZBM is increasing suddenly as soon as $|B| > 2$ mT.

To describe the relation between the width of the ZBM and the applied magnetic field, we use the pair breaking parameter $\alpha = eDB$, which is relevant for thin superconducting films in a perpendicular magnetic field (see, e.g., Ref. 31). In the experiment presented here, the magnetic field is oriented perpendicular to the surface 2DEG, where superconducting correlations are induced. Thus, as a first approximation the expression for α can be applied for the system discussed here. Since the width of the ZBM is given by approximately the Thouless energy, we expect that as soon as α is becoming larger than the width of the zero bias maximum at zero magnetic field [$eV_{ZBM}(B=0)$], the width V_{ZBM} should be given by α/e . This means that for fields above a threshold value B_{th} , the width V_{ZBM} is expected to increase linearly with B according to the relation $V_{ZBM}(B) = DB$.

A magnetic pair-breaking length l_B can be introduced by defining the criterion $\alpha = \varepsilon_g(l_B)$ ($= \hbar D/l_B^2$). This yields $l_B = \sqrt{\Phi_0/\pi B}$, where Φ_0 is the magnetic flux quantum. With increasing B , the magnetic pair-breaking length is decreased. l_B can be considered as effective length L_{eff} of the sample. Thus, our approach is in close analogy to the discussion of the magnetic-field-dependent phase-breaking length by Charlat *et al.*⁹ (see above). The threshold field B_{th} will be defined from the criterion $l_B = L$. From this, B_{th} is given by $B_{\text{th}} = \Phi_0/\pi L^2$. With $L = 500$ nm, one obtains $B_{\text{th}} = 2.5$ mT, which is in very good agreement with the experimental data.

Figure 8 shows the width of the ZBM (V_{ZBM}) as a function of B . The solid circles indicate the measurement points. For $2 \text{ mT} < |B| < 10 \text{ mT}$, V_{ZBM} is increasing linearly with B . The dependence V_{ZBM} on B can be approximated by aB ,

where a is found to be $a \approx \pm 90 \mu\text{V}/\text{mT}$. From the theoretical arguments discussed above, a linear increase of V_{ZBM} ($V_{\text{ZBM}} = DB$, $D \approx 47 \mu\text{V}/\text{mT}$) is expected. Thus, the experimentally found linear dependence of V_{ZBM} is consistent with the theoretical consideration. On the other hand, the experiment yields for a a value which is a factor of 2 larger than expected from these simple theoretical arguments based on pair breaking in superconducting surface films.

E. Comparison of the Nb/Au step junctions with Au/Au step junctions, Nb/Nb step junctions, and large-distance Nb/Au junctions

To ensure that the discussed peculiarities are due to the influence of the superconductor on the 2DEG, we investigated step junctions with two Au electrodes (instead of one Nb and one Au electrode) at low temperatures. The junctions have been prepared using the same fabrication parameters as described above for the Nb/Au junctions. For the same temperature region ($300 \text{ mK} < T < 12 \text{ K}$) and voltage range ($-3 \text{ mV} < V < 3 \text{ mV}$), the Au/Au junctions show different behavior compared to the Nb/Au junctions. The differential resistance of the Au/Au junctions depends only weakly on the current, magnetic field, and temperature. A very broad ($\approx 5 \text{ mV}$), flat ($R_0/R_n \approx 1.01$) resistance enhancement around zero bias is detected. The dV/dI curve is similar to the dV/dI curves of Nb/Au step junctions for high fields shown in Fig. 7(b). Also the values of the resistances are of the same order of magnitude as for the Nb/Au step junctions.

With Nb/Nb step junctions ($L \approx 200 \text{ nm}$), we observe Josephson coupling or at least enhanced conductivity around zero bias. Results with Nb-InAs-Nb step junctions with a rather low interface transparency are published in Refs. 32 and 33. With improved interface cleaning (low energy Ar-ion treatment), the Nb-InAs-Nb junctions have a normal resistance close to the resistance of the Nb-InAs-Au step junctions presented here.³⁴ The dV/dI curves show an asymmetry of the same order of magnitude (about 2%) as the Nb/Au step junctions.

Furthermore, to ensure that the occurrence of the large zero-bias-resistance enhancement is not only due to the influence of the superconductor, but also due to a small distance between the superconducting and normal conducting reservoir, we investigated planar junctions where the distance between the normal conducting and superconducting electrode was approximately $100 \mu\text{m}$. In this case, effects due to phase coherence do not play a role any more. Here, we observe again the typical, ‘‘macroscopic’’ InAs characteristics, with a broad (several mV), flat ($R_0/R_n \approx 1.01$) resistance enhancement around zero bias [comparable to the curves for high fields shown in Fig. 7(b)]. Similar characteristics are observed with the family of step junctions described here, after the channel length has been increased to about $1 \mu\text{m}$ by additional etching of the semiconductor.

IV. CONCLUSIONS

We have measured the temperature, current, and magnetic field dependence of the current-voltage characteristics in Nb-InAs-Au step junctions with a distance between the Nb and Au electrodes of about 500 nm . An increase of the system’s resistance is observed when all energies involved are below the Thouless energy of the sample. Our experimental results are compared to recent theories developed for proximity induced correlations in diffusive, quasi-one-dimensional normal metals. The good agreement between experiment and theory suggests that the reentrance effect of normal conductivity plays an important role for systems based on a two-dimensional electron gas in the diffusive limit.

ACKNOWLEDGMENTS

We would like to thank A. Kastalsky for his contribution in the early stage of this work. We are grateful to A.I. Braginski, T. Doderer, E. Goldobin, H. Kohlstedt, M.Yu. Kupriyanov, H. Lüth, K. Neurohr, T. Schäpers, and A.V. Ustinov for many valuable suggestions and discussions, and to Ch. Krause for the MBE growth of the semiconductors.

*Permanent address: Institute of Solid State Physics, Chernogolovka, Moscow District, 142432, Russia. Present address: Faculty of Applied Physics, Low Temperature Division, University of Twente, P.O. Box 217, 7500 AE Enschede, The Netherlands.

¹ *Mesoscopic Superconductivity*, edited by F. W. J. Hekking, G. Schön, and D. V. Averin (Elsevier, Amsterdam, 1994).

² S. N. Artemenko, A. F. Volkov, and A. V. Zaitsev, *Solid State Commun.* **30**, 771 (1979).

³ A. Volkov, N. Allsopp, and C. J. Lambert, *J. Phys.: Condens. Matter* **8**, L45 (1996).

⁴ Yu.V. Nazarov and T. H. Stoof, *Phys. Rev. Lett.* **76**, 823 (1996); T. H. Stoof and Yu.V. Nazarov, *Phys. Rev. B* **53**, 14 496 (1996).

⁵ A. A. Golubov, F. K. Wilhelm, and A. D. Zaikin *Phys. Rev. B* **55**, 1123 (1997).

⁶ P. W. Brouwer and C. W. J. Beenakker, *Phys. Rev. B* **52**, 3868 (1995).

⁷ C. W. J. Beenakker, *Rev. Mod. Phys.* **69**, 731 (1997).

⁸ A. Barone and G. Paternò, *Physics and Applications of the Josephson Effect* (Wiley, New York, 1982).

⁹ P. Charlat, H. Courtois, Ph. Gandit, D. Maily, A. F. Volkov, and B. Pannetier, *Czech. J. Phys.* **46**, 3107 (1996).

¹⁰ P. Charlat, H. Courtois, Ph. Gandit, D. Maily, A. F. Volkov, and B. Pannetier, *Phys. Rev. Lett.* **77**, 4950 (1996).

¹¹ V. T. Petrashov, V. N. Antonov, P. Delsing, and T. Claeson, *Phys. Rev. Lett.* **74**, 5268 (1995).

¹² S. Gueron, H. Pothier, N. O. Birge, D. Esteve, and M. Devoret, *Phys. Rev. Lett.* **77**, 3025 (1996).

¹³ S. G. den Hartog, C. M. A. Kapteyn, B. J. van Wees, T. M. Klapwijk, and G. Borghs, *Phys. Rev. Lett.* **77**, 4957 (1996).

¹⁴ H. Takayanagi and T. Kawakami, *Phys. Rev. Lett.* **54**, 2449 (1985).

¹⁵ H. Kroemer, C. Nguyen, E. L. Hu, E. L. Yuh, M. Thomas, and K. C. Wong, *Physica B* **203**, 298 (1994).

¹⁶ A. Chrestin, T. Matsuyama, and U. Merkt, *Phys. Rev. B* **55**, 8457 (1997).

¹⁷ T. Ando, A. B. Fowler, and F. Stern, *Rev. Mod. Phys.* **54**, 437 (1982).

¹⁸ A. Kastalsky, *Hybrid Devices, Particular Josephson Transistors*, patent, submitted to U.S. and German Patent offices (Dec. 1995, Nov. 1996).

- ¹⁹O. M. Corbino, Phys. Z. **14**, 561 (1911).
- ²⁰Inés Friedrich, thesis, Rheinisch-Westfälische Technische Hochschule Aachen 1997.
- ²¹E. Yamaguchi, Phys. Rev. B **32**, 5280 (1985).
- ²²M. F. Millea, A. F. Silver, and L. D. Flesner, Thin Solid Films **56**, 253 (1979).
- ²³P. H. C. Magnée, S. G. den Hartog, B. J. van Wees, T. M. Klapwijk, W. van de Graaf, and G. Borghs, Appl. Phys. Lett. **67**, 3569 (1995).
- ²⁴G. E. Blonder, M. Tinkham, and T. M. Klapwijk, Phys. Rev. B **25**, 4515 (1982).
- ²⁵A. F. Volkov, A. V. Zaitsev, and T. M. Klapwijk, Physica C **210**, 21 (1993).
- ²⁶From the parameters determined in Corbino geometry ($R_{\square} = 1.16 \text{ k}\Omega$), one expects a channel resistance $R_{\text{ch}} = R_{\square}(L/W)$ of approximately 5.8Ω . Any additional contact resistance R_c would increase R_n further. Our measured resistance is smaller than this value (see Table I). This effect is commonly observed with Nb/InAs/Nb junctions (Refs. 14,27–29). One possible reason for this reduction is the contribution of shunting current paths on either side of the junction.
- ²⁷H. Takayanagi, J. Bindslev Hansen, and J. Nitta, Phys. Rev. Lett. **74**, 162 (1995).
- ²⁸B. J. van Wees, A. Dimoulas, J. P. Heida, T. M. Klapwijk, W. v. d. Graaf, and G. Borghs, in *Mesoscopic Superconductivity* (Ref. 1).
- ²⁹P. H. C. Magnee, Ph.D. thesis, University Groningen, 1996.
- ³⁰U. Kunze, Z. Phys. B **76**, 463 (1989).
- ³¹K. Maki, in *Superconductivity*, edited by R. D. Parks (Dekker, New York, 1969), p. 1035.
- ³²S. G. Lachenmann, A. Kastalsky, I. Friedrich, A. Förster, A. V. Ustinov, and D. Uhlisch, Czech. J. Phys. **46**, 659 (1996).
- ³³S. G. Lachenmann, A. Kastalsky, I. Friedrich, A. Förster, and D. Uhlisch, J. Low Temp. Phys. **106**, 321 (1997).
- ³⁴S. G. Lachenmann, I. Friedrich, D. Uhlisch, A. Förster, A. Kastalsky, and A. A. Golubov (unpublished).